

This is the accepted manuscript made available via CHORUS. The article has been published as:

# Charging-assisted hydrogen release mechanism in layered boron hydride

Tesfaye A. Abtew and Peihong Zhang

Phys. Rev. B **84**, 094303 — Published 14 September 2011

DOI: [10.1103/PhysRevB.84.094303](https://doi.org/10.1103/PhysRevB.84.094303)

# Charging Assisted Hydrogen Release Mechanism in Layered Boron Hydride

Tesfaye A. Abtew\* and Peihong Zhang†

Department of Physics, University at Buffalo, State University of New York, Buffalo, New York 14260, USA

(Dated: August 30, 2011)

We present a first principles study of the dehydrogenation mechanism of a recently proposed layered boron hydride ( $B_2H_2$ ) for hydrogen storage. The nudged elastic band method is employed to study the kinetic energy barrier against the release of hydrogen. Introducing additional charges in to the  $B_2H_2$  system reduces the electron deficiency of boron layer thereby lowering the dehydrogenation kinetic energy barrier. Finite temperature molecular dynamics simulation further confirms the release of hydrogen atoms and the formation of molecular hydrogen upon charging the system. The boron network remains intact throughout the simulation up to at least 500 K. These results suggest a charging assisted dehydrogenation mechanism in this system.

PACS numbers: 71.15.Pd, 74.70.Ad, 88.30.R

## I. INTRODUCTION

The hydrogen storage challenge impedes the broad application of this otherwise compelling energy carrier. Despite the sheer number of materials investigated and proposed so far,<sup>1–8</sup> practical on-board hydrogen storage remains one of the major obstacles to fully utilizing hydrogen based fuel cells for transportation.<sup>9</sup> This is because on-board vehicular hydrogen storage has strict demands on various aspects such as safety, cost, volumetric and gravimetric energy density, thermodynamic efficiency, and kinetics and reversibility.<sup>10–12</sup> One of the key requirements for any hydrogen storage material is its ability to release hydrogen at practical temperature and pressure. As a result, thermodynamically, an ideal material for hydrogen storage must lie near the hydrogenation/dehydrogenation phase boundary. This stringent requirement is unlikely to be satisfied with materials involving only conventional interaction mechanisms (e.g., covalent, ionic, or van der Waals), and there is increasing interest in exploring unconventional and intermediate bonding mechanisms<sup>13–19</sup> in the search for hydrogen storage materials.

Fortunately, hydrogen, although being the simplest element, has a surprisingly rich chemistry. In addition to forming conventional covalent and ionic bonds, hydrogen also forms various intermediate-strength bonds in many compounds and structures, including the widely studied Kubas interaction<sup>19,20</sup> between hydrogen and transition metals in many dihydrogen complexes. On the other hand, boron also has an extremely rich and flexible chemistry. The rich chemistry of boron and hydrogen provides compelling opportunities to search for new boron-hydrides for on-board hydrogen storage. Recently, we proposed<sup>22</sup> that the three-center two-electron ( $3c2e$ )<sup>23</sup> boron-hydrogen bonds found in many boranes may be able to stabilize the planar boron structure to form layered solid  $B_2H_2$  as shown in Fig. 1. The  $3c2e$  B–H bonds have also been proposed to stabilize BH fullerene structures.<sup>21</sup> This structure is isoelectronic to  $MgB_2$  and can be doped with electrons. Charge may be introduced to the system through alkali metal intercalation or a boron self-doping mechanism.<sup>22</sup> We have investigated the electronic and dynamical properties of  $B_2H_2$  and showed that the structure is dynamically stable. We have also studied the effects of charging on the dynamical properties of  $B_2H_2$  and found that some hydrogen related phonon modes are softened significantly, whereas boron modes are either hardened or not strongly affected. This finding suggests a charging-assisted hydrogen release mechanism.

In this paper, we extend our work to address the hydrogen release dynamics and kinetics by carrying out *ab initio* molecular dynamics (MD)<sup>24</sup> simulations and nudged elastic band (NEB)<sup>25</sup> calculations. We have investigated both neutral and electron doped systems and found that charging the  $B_2H_2$  structure with electrons significantly lowers the dehydrogenation kinetic energy barrier and facilitates the release and possible formation of hydrogen molecules. The underlying boron backbone structure, in contrast, remains intact.

## II. COMPUTATIONAL DETAILS

The density functional theory<sup>26</sup> calculations in the present work are performed using the QUANTUM ESPRESSO<sup>27</sup> package. The generalized gradient approximation of Perdew, Burke, and Ernzerhof<sup>28</sup> is used for the exchange and correlation energy. Ultrasoft pseudopotentials<sup>29</sup> are used to describe the electron–ion interactions. The kinetic energy cutoff for the plane wave expansion of the wave functions is set at 50 Ry and that for charge density expansion is 500 Ry. A Nudged Elastic Band (NEB)<sup>25</sup> method implemented in the QUANTUM ESPRESSO package<sup>27</sup> is used to compute the kinetic energy barrier. In the NEB calculations, we have used a climb-image method, in which we have used an enough number of images (10 images to discretize the path). At each NEB step, we make sure that the

norm of the forces orthogonal to the path is less than the threshold value of 0.05 eV/Å on the individual images. The initial and final structures are well relaxed before the NEB calculation. To increase the resolution around the saddle point, we used a variable elastic constant scheme. Thermodynamic stability and charging assisted hydrogen release are then investigated using Car-Parrinello molecular dynamics (CPMD)<sup>24</sup> simulations. For the molecular dynamics calculations, we have used a double layer supercell structure with a total of 288 atoms. In the CPMD calculation, the ionic temperature is controlled using a Nosé-Hoover thermostat.<sup>30,31</sup> Oscillation frequency of the thermostat is chosen by taking an average vibration mode of the system to excite as many modes as possible. For the electronic properties and NEB calculations, a  $k$ -point sampling of  $12 \times 12 \times 4$  is used. However, for the CPMD simulation, a  $\Gamma$  point sampling of the supercell is used.

### III. STRUCTURAL AND ELECTRONIC PROPERTIES

Figure 1 shows the proposed layered boron hydride  $B_2H_2$ . Boron atoms in  $B_2H_2$  form borane-like three-center two-electron (3c2e) bonds<sup>23</sup> with bridging hydrogen atoms and connect to other in-plane boron atoms via a conventional  $sp^2$  hybridization. The hydrogen atoms are weakly bound to the hexagonal boron plane in pairs, one above, and the other below the plane as shown in Fig. 1. The weakly bonded hydrogens are crucial to stabilize the boron network and are desirable for the release of hydrogen at practical conditions. The detailed structural information of this model has been discussed in our recent paper.<sup>22</sup>

The electronic structure of this system has close resemblance with that of  $MgB_2$  with some differences. For instance, in the case of  $B_2H_2$ , the degeneracy of the  $p\sigma$  bands at the  $\Gamma$ -point is removed due to the lowering of the symmetry from  $D_{6h}$  to  $D_{2h}$ . Consequently, only one of the  $p\sigma$  bands crosses the Fermi level and the hole pocket near the  $\Gamma$ -point comes from the upper  $p\sigma$  band. Furthermore, the degeneracy of the  $p\pi$  bonding and antibonding states near the Fermi level is also removed. The Fermi surface of  $B_2H_2$  consists of both a  $p\sigma$  derived hole pocket and a  $p\pi$  derived electron pocket, which is similar to that of  $MgB_2$ .

The electronic structure of the  $B_2H_2$  system is further analyzed using the projected density of states (PDOS) which is shown in Fig. 2. The PDOS shows significant involvement of the hydrogen  $s$  states in the bonding. The electronic states near the Fermi level are derived from bonding B- $p_y$  and anti-bonding B- $p_z$  states. These states determine how the boron-boron and hydrogen-boron bonds respond when additional electrons are introduced into the system. At low charging levels, electrons occupy both the bonding B- $p_y$  and anti-bonding B- $p_z$  states. As a result, the boron network is further stabilized and the energy of boron stretching mode along the  $y$ -direction increases with charging at a low charging level.<sup>22</sup> Occupying the anti-bonding B- $p_z$  states, on the other hand, tends to soften other related phonon modes. As the charging level increases, electrons continue occupying the anti-bonding B- $p_z$  states, and eventually the anti-bonding H- $s$  states. Although the system is still dynamically stable at a relatively high charging level, thermodynamically it may prefer to release hydrogen in exchange for stabilizing the boron network. In the next section, we investigate the charging effects on the hydrogen release kinetic energy barrier.

### IV. CHARGING EFFECTS ON DEHYDROGENATION KINETIC ENERGY BARRIER: AN NEB STUDY

The electron deficient hexagonal boron layer could be stabilized through the formation of 3c2e with hydrogen. Therefore, when the boron layer acquires extra electron (through doping or charging), it becomes less electron deficient. This in turn weakens the bridge hydrogen-boron bonds. Consequently, as the boron layer gets enough electrons to quench its electron deficiency, the hydrogen will no longer bound to the boron layer and gets released. One possibility of making (and regenerating)  $B_2H_2$  is through atomic exchange with metal diborides such as  $Li_2B_2$  as follows:  $\alpha-Li_2B_2 + H_2 \longleftrightarrow 2Li + B_2H_2$ . Interestingly, the calculated separation between the boron hydride layer is about 4.0 Å, which is large enough to accommodate lithium ions. This raises an intriguing possibility of coupling hydrogenation/dehydrogenation with Li intercalation/extraction. In other words, the hydrogenation/dehydrogenation process may be assisted by a Li-ion battery setup.

In the  $B_2H_2$  structure, hydrogen atoms are bound to the hexagonal boron plane in pairs, one above, and the other below the plane. These bridge hydrogen atoms serve as electron donors and stabilize the electron deficient boron layer. Therefore, dehydrogenation will destabilize the hexagonal boron layer. To preserve the boron network, additional charges (electrons) must be introduced to the system. In fact, as it will be shown later, it is very difficult to release hydrogen from the neutral  $B_2H_2$  structure and therefore charging is a promising way to tune the strength of the B-H bonds and to facilitate the release of hydrogen. Charges (electrons) can be introduced to the  $B_2H_2$  structure by alkali atom intercalation or through a boron self-doping mechanism.<sup>32,33</sup>

There are many possible pathways for a hydrogen atom to detach itself from the boron plane and to recombine with another hydrogen to form  $H_2$ . The presence of numerous pathways makes it difficult to identify and model a realistic hydrogen release mechanism with the NEB method.<sup>25</sup> However, qualitative information regarding the kinetic energy barrier as well as effects of charge doping can be obtained by considering selected hydrogen release pathways. Here we consider two different hydrogen release pathways and investigate the charging effects on the dehydrogenation kinetic energy barrier.

First, we consider a scenario in which hydrogen atoms are released from two adjacent self-doped  $B_2H_2$  layers shown in Fig. 3(a) and diffuse to merge together to form  $H_2$  as shown in Fig. 3(b). Here we borrow the concept of self-doping as introduced by Tang *et al.*<sup>32</sup> and consider a low self-doping system, a  $B_{33}H_{32}$  bi-layer structure. Before we discuss the kinetic energy barrier associated with such a configuration, we calculate its formation energy and compare it with an undoped  $B_{32}H_{32}$  structure. The formation energy is calculated using a super cell model. We compare the calculated energy of  $B_{33}H_{32}$  with that of  $B_{32}H_{32} + B$  (solid alpha boron) and find that it is indeed energetically favorable to introduce a self-doped boron to the system:  $\Delta E = E[B_{32}H_{32}] + E[B(\text{solid alpha boron})] \rightarrow E[B_{33}H_{32}]$ . The energy gain,  $\Delta E$ , is about 1.96 eV per boron atom. In the dilute limit, we estimated that the energy gain is about 2.4 eV per boron atom.

The calculated kinetic energy barrier for both a neutral ( $B_{32}H_{32}$ ) and a self-doped ( $B_{33}H_{32}$ ) systems is shown in Fig. 3(c). As it is shown in the figure, it is clear that releasing hydrogen from the neutral  $B_2H_2$  system would be very difficult. However, with the presence of a self-doped boron, the kinetic energy barrier is significantly reduced. The additional boron donates electrons to the  $B_2H_2$  sheet, which makes the system less electron deficient and weakens the bridge B–H bonds, thereby facilitating the hydrogen release. Therefore, one may use charging (in this case, through self-doping) to tune the strength of the B–H bridge bonds and the dehydrogenation kinetic energy barrier.

The second scenario that we consider involves the release of hydrogen and formation of  $H_2$  from a single  $B_2H_2$  layer as shown in Fig. 4. Again, we have studied both a neutral and an electron doped systems. In the case of electron doping, we introduce one additional electron per unit cell so that the system is isoelectronic to  $AlB_2$ . The additional charge is balanced by a uniform positive background. Practically, the additional charges can be introduced by incorporating electron donors like lithium (Li) into the  $B_2H_2$  structure. The calculation is much more involved in this case since we have to explore a two-dimensional energy surface. To characterize the energy barrier, we have examined the energy profile of a single layer  $B_2H_2$  structure by considering different hypothetical paths over which the H–B bridge bonds are broken to form  $H_2$ . The calculation is performed using NEB by fixing the hydrogen atoms at a given point along the z-axis and allowing the two hydrogen atoms to move along the y-axis. Along the y-axis, the H–H distance is allowed to change from the initial value of 3.0 Å to 0.7 Å. By analyzing the calculated energy profile, we find a minimum energy path for the formation of  $H_2$  molecule as shown in Fig. 4(b). We again observed significant lowering (by about 1.5 eV) of the dehydrogenation kinetic energy barrier when additional charges (electrons) are introduced to the system.

In both of the dehydrogenation pathways considered above, we find that the kinetic energy barrier is lowered significantly as a result of charge doping. It is also possible that the two charge doping mechanisms (i.e., boron self-doping and alkali metal intercalation) may be combined to achieve optimal results. While boron self-doping may serve as a convenient means to pre-tune the strength of the B–H bonds, alkali atom intercalation may be introduced at the time of dehydrogenation. This brings an interesting possibility of utilizing the electrochemical reactions to facilitate the dehydrogenation process. It may also be interesting to investigate the possibility of combining the Kubas interaction mechanism<sup>19</sup> with the B–H 3c2e bonding mechanism<sup>23</sup> to fine tune the dehydrogenation kinetics and thermodynamics of boron hydride solids.

## V. CHARGING ASSISTED HYDROGEN RELEASE: A MOLECULAR DYNAMICS SIMULATION STUDY

To further unravel the charging effects on the thermodynamics of the layered  $B_2H_2$  structure and its dehydrogenation kinetics, we have performed an extensive Car-Parrinello molecular dynamics<sup>24</sup> simulations for both neutral and charged  $B_2H_2$  systems. We use a 288 atoms double layer supercell structure of  $B_2H_2$  for our MD calculations. The newly formed structure is then relaxed before the simulation. For the system size we considered here (288 atoms), the calculations become very time consuming. This is because the small mass of hydrogen requires an extremely small time step (0.025 fs used in this study) to integrate the equations of motion. Despite these issues, we have performed a long-time simulation of more than 10 ps with a time step of 0.025 fs using 400,000 MD steps both for the neutral and charged  $B_2H_2$ . Here we would like to emphasize the fact that in many cases, molecular dynamics simulations of few ps are found to be sufficient to obtain qualitative understanding of the dynamics of the system. From that perspective, we believe that the 10 ps time step is enough to offer some insight into the charging assisted hydrogen release mechanism in this system.

### A. Neutral System

To analyze the thermodynamic stability of the  $B_2H_2$  structure, we have performed CPMD simulations at different temperatures (300 K, 400 K and 500 K). Figure 5 shows a snapshot of the  $B_2H_2$  structure taken after an MD simulation time of 3.5 ps at 500 K. It is clear that hydrogen atoms remain tightly bound to the boron framework and the boron layer remains intact. Consequent snapshots of the  $B_2H_2$  structure at different simulation time steps (as well as at different temperatures) up to 10 ps show similar structural arrangements without any significant weakening of the hydrogen-boron bridge bonds.

To further characterize the structural changes for the neutral  $B_2H_2$  structure, we have also tracked various atomic distances (or bond lengths) throughout the simulation to analyze the possibilities of bond breaking and the formation of molecular hydrogens. Figure 6 shows the calculated atomic distance distribution for boron-boron, boron-hydrogen and hydrogen-hydrogen at  $T=500$  K. These distances are calculated at each MD step and the histogram, which is normalized to unity, represents the bond lengths distribution over the simulation time. Before the MD simulation, the initial nearest neighbor boron-boron (B–B) distances were 1.8 Å and 1.7 Å and the hydrogen-boron (H–B) distance was 1.3 Å. The inter-layer H–H distance between was 1.3 Å. After the MD simulation, as can be seen from Fig. 6, the H–H distance distribution is significantly broadened, indicating a large fluctuation of the positions of hydrogen atoms. In contrast, broadening of the B–B distance is significantly smaller, which again suggests the rigidity of the boron network. These results show that  $B_2H_2$  structure is sufficiently stable at least up to 500 K and that the strength of the B–H bridge bonds are indeed intermediate. However, we do not observe the release of hydrogen atoms or the formation of hydrogen molecules at the simulation temperatures.

### B. Charged System

As discussed in the previous sections, the B–H bridge bond in the  $B_2H_2$  structure is formed as a result of electron deficiency of the underlying hexagonal boron sheet. As the boron layers acquire extra electrons, they become less electron deficient and the strength of these B–H bonds can be significantly weakened. This may allow the release of hydrogen at practical temperatures. We have carried out CPMD simulations for the charged system with one additional electron per unit cell. The simulation is performed on the same structure and conditions as in the case of the neutral system discussed above. Unlike the case of the neutral  $B_2H_2$  structure, the simulations for the charged system show considerable structural rearrangements. Figure 7 shows a snapshot of the  $B_2H_2$  structure at  $T=500$  K, which reveals considerable rearrangements in the H–B bridge bonds and the formation of an  $H_2$  molecule.

By analyzing the atomic distances (bond lengths) as we did for the neutral system, we made the following observations: (a) The H–B bridge bonds are weakened significantly and occasionally break during the simulation period. The broken B–H bonds sometimes result in the release of hydrogen atoms, which may combined with another hydrogen to form  $H_2$  molecules. Sometimes the broken bridge bond simply result in single B–H bond. (b) Like the neutral system, the boron plane remains intact. In Fig. 8, we show the bond distance distribution for B–B, B–H, and H–H for the charged  $B_2H_2$  structure at  $T=500$  K. The higher simulation temperature smears out the two B–B bond lengths so that the B–H bond length distribution shows only one peak. However, the boron network still remains intact, again confirming stability of the boron plane. Unlike the neutral system, the H–H distance distribution shows a significant number of counts at small (less than 1.0 Å) H–H distances. When the H–H distances gets smaller than 1.0 Å, it is very likely that a molecular hydrogen will form. In fact, we observe a peak in the H–H distance distribution around 0.75 Å which corresponds to the formation of hydrogen molecules. These results clearly indicate the presence of weakly bonded and unbonded hydrogen atoms and the formation of hydrogen molecules during the simulation period, a feature that was not seen in the simulation of the neutral system. Therefore, the presence of extra charge leads to significantly weakened B–H bridge bonds, which suggests a charging assisted dehydrogenation mechanism.

## VI. CONCLUSION

We presented an *ab initio* study of hydrogen release mechanism in layered  $B_2H_2$  system. We have investigated the charging effects on the dehydrogenation kinetic energy barrier for two possible hydrogen release pathways. The additional charges introduced into the  $B_2H_2$  system reduce the electron deficiency of boron network and thereby modulate the strength of the B–H bridge bonds and dehydrogenation kinetic barriers. As a result, for both dehydrogenation pathways, we find a significant decrease in the energy barrier required for hydrogen release upon charge doping. We have also carried out finite temperature MD simulation both for the neutral and charged  $B_2H_2$  supercell structures. Our MD result shows a significant weakening and breaking of the B–H bonds with charging, which suggests a charging assisted dehydrogenation mechanism. The boron framework remains stable for both the neutral and charged systems

at least up to 500 K. The stabilization of the electron deficient boron network by additional charges is desirable to preserve the boron framework through dehydrogenation cycle. Boron self doping as well as alkali atom intercalation can be used as a means of introducing extra charges to the system to tune the strength of the B–H bonds. This brings an interesting possibility of utilizing the electrochemical reactions to facilitate the dehydrogenation process.

## VII. ACKNOWLEDGMENTS

This work was supported by the National Science Foundation through Grant No. CBET-0844720, and by the donors of the American Chemical Society Petroleum Research Fund. We acknowledge the computational support provided by the Center for Computational Research at the University at Buffalo, SUNY.

- 
- \* Electronic address: [tesfayea@buffalo.edu](mailto:tesfayea@buffalo.edu)  
 † Electronic address: [pzhang3@buffalo.edu](mailto:pzhang3@buffalo.edu)
- <sup>1</sup> B. Bogdanovic, R. A. Brand, A. Marjanovic, M. Schwickardi and J. Tolle, J. of Alloys and Compounds **302**, 36 (2000).
  - <sup>2</sup> A. Zuttel, P. Wenger, S. Rentsch, P. Sudan, P. Mauron, and C. Emmenegger, J. of Power Sources **118**, 1 (2003).
  - <sup>3</sup> P. Chen, Z. Xiong, J. Luo, J. Lin, and K. Tan, Nature (London) **420**, 302 (2002).
  - <sup>4</sup> L. Hornekaer, E. Rauls, W. Xu, Z. Sljivancanin, R. Otero, I. Stensgaard, E. Laegsgaard, B. Hammer, and F. Besenbacher, Phys. Rev. Lett. **97**, 186102 (2006).
  - <sup>5</sup> Y. H. Kim, Y. F. Zhao, A. Williamson, M. J. Heben, and S. B. Zhang, Phys. Rev. Lett. **96**, 16102 (2006).
  - <sup>6</sup> N. L. Rosi, J. Eckert, M. Eddaoudi, D. T. Vodak, J. Kim, M. O’Keeffe, O. M. Yaghi, Science, **300**, 1127 (2003).
  - <sup>7</sup> A. Gutowska, L. Y. Li, Y. S. Shin, C. M. M. Wang, X. H. S Li, J. C. Linehan, R. S. Smith, B. D. Kay, B. Schmid, W. Shaw, M. Gutowski, and T. Autrey, Angew. Chem. Int. Ed. **44**, 3578 (2005).
  - <sup>8</sup> T. K. Hoang and D. M. Antonelli, Adv. Mater. **21**, 1787 (2009).
  - <sup>9</sup> G. W. Crabtree, M. S. Dresselhaus, and M. V. Buchanan, Physics Today **57**, 39 (2004).
  - <sup>10</sup> [[http://www.hydrogen.energy.gov/annual\\_review.html](http://www.hydrogen.energy.gov/annual_review.html)].
  - <sup>11</sup> S. Satyapal, J. Petrovic, C. Read, G. Thomas, and G. Ordaz, Catalysis Today **120**, 246 (2007).
  - <sup>12</sup> L. Schlapbach and A. Zuttel, Nature (London) **414**, 353 (2001).
  - <sup>13</sup> H. Lee, J. Ihm, M. L. Cohen, and S. G. Louie, Nano Lett. **10**, 793 (2010).
  - <sup>14</sup> L. Wang, K. Lee, Y. Y. Sun, M. Lucking, Z. F. Chen, J. J. Zhao, and S. B. B. Zhang, ACS Nano **3**, 2995 (2009).
  - <sup>15</sup> M. Yoon, S. Yang, C. Hicke, E. Wang, D. Geohegan, and Z. Zhang, Phys. Rev. Lett. **100**, 206806 (2008).
  - <sup>16</sup> T. Yildirim and S. Ciraci, Phys. Rev. Lett. **94**, 175501 (2005).
  - <sup>17</sup> Y. Zhao, Y.-H. Kim, A. C. Dillon, M. J. Heben, and S. B. Zhang, Phys. Rev. Lett. **94**, 155504 (2005).
  - <sup>18</sup> T. Hoang, M. I. Webb, H. V. Mai, A. Hamaed, C. J. Walsby, M. Trudeau, D. M. Antonelli, J. Am. Chem. Soc. **132**, 11792 (2010).
  - <sup>19</sup> G. J. Kubas, R. R. Ryan, B. I. Swanson, P. J. Bergamini, H. J. Wasserman, J. Am. Chem. Soc. **106**, 451 (1984).
  - <sup>20</sup> G. J. Kubas, J. Organomet. Chem. **35**, 37 (2001).
  - <sup>21</sup> A. A. Quong, M. R. Pederson and J. Q. Broughton Phys. Rev. B **50**, 4787 (1994).
  - <sup>22</sup> T. A. Abtew, B. Shih, P. Dev, V. H. Crespi, and P. Zhang, accepted, Phys. Rev. B (2011).
  - <sup>23</sup> W. N. Lipscomb, *Boron Hydrides* (W. A. Benjamin, INC, New York, 1963).
  - <sup>24</sup> R. Car and M. Parrinello, Phys. Rev. Lett. **55**, 2471 (1985).
  - <sup>25</sup> G. Henkelman and H. Jonsson, J. Chem. Phys. **113**, 9978, (2000).
  - <sup>26</sup> W. Kohn and L. J. Sham, Phys. Rev. **140**, A1133 (1965).
  - <sup>27</sup> P. Giannozzi *et al.*, J. Phys. Condens. Matter **21**, 395502 (2009).
  - <sup>28</sup> J. P. Perdew, K. Burke, and M. Ernzerhof, Phys. Rev. Lett. **77**, 3865 (1996).
  - <sup>29</sup> D. Vanderbilt, Phys. Rev. B **41**, 7892 (1990).
  - <sup>30</sup> S. Nosé, J. Chem. Phys. **81**, 511 (1984).
  - <sup>31</sup> W. Hoover, Phys. Rev. A **31**, 1695 (1985).
  - <sup>32</sup> H. Tang and S. Ismail-Beigi, Phys. Rev. Lett. **99**, 115501 (2007).
  - <sup>33</sup> E. Suleyman, G. A. de Wijs, and G. Brocks, J. Phys. Chem. C **113**, 18962 (2009).

## Figures



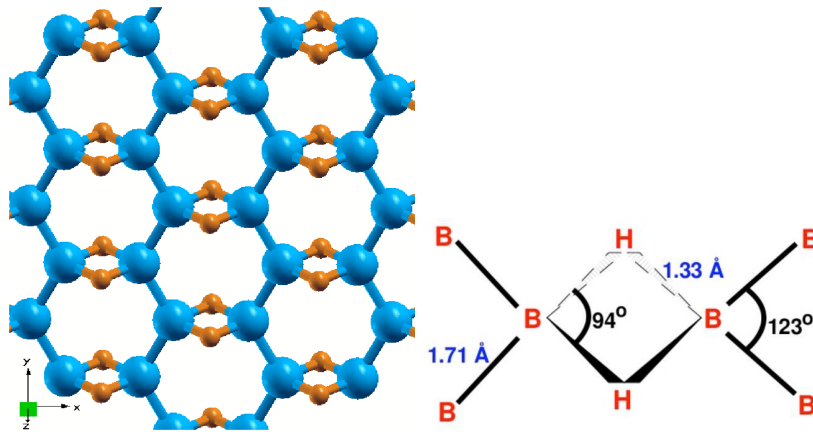


FIG. 1: (Color online) Structure of single-layer  $B_2H_2$  and the corresponding bond angles and bond lengths. Boron is blue (big spheres) and hydrogen is orange (small spheres).



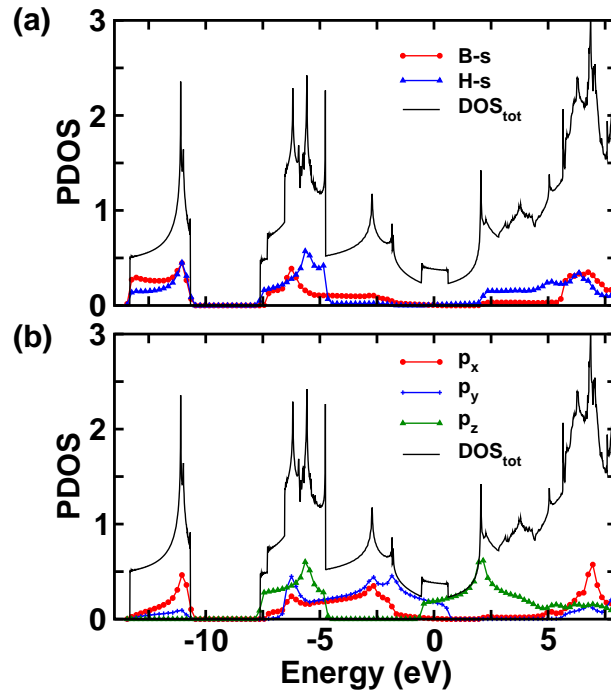


FIG. 2: (Color online) Projected density of states (PDOS) and total density of states (DOS<sub>tot</sub>) of single-layer B<sub>2</sub>H<sub>2</sub>. (a) PDOS for B 2s and H 1s; and (b) PDOS for B-2p<sub>x</sub>, B-2p<sub>y</sub> and B-2p<sub>z</sub>. The Fermi level is at 0 eV. Units are in states/eV/cell.

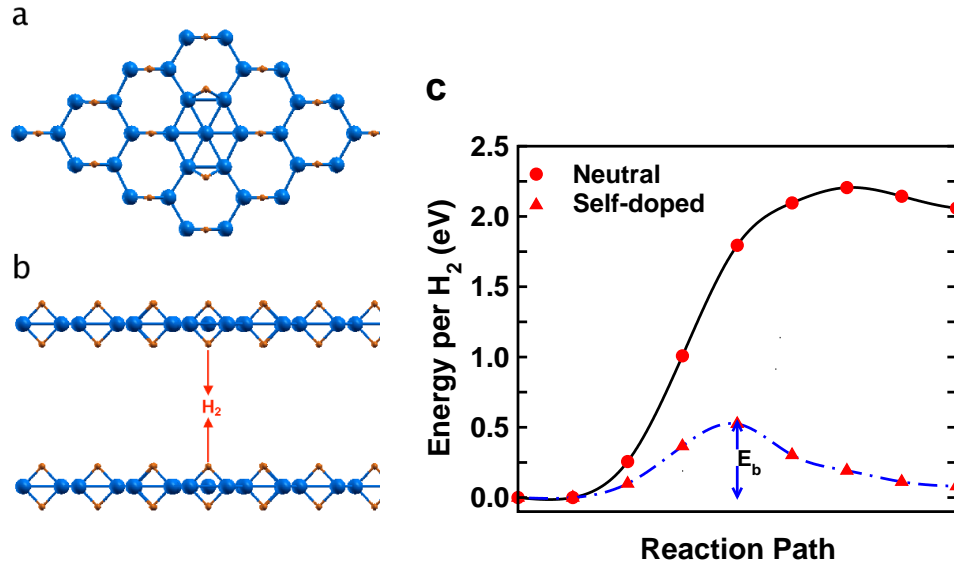


FIG. 3: (Color online) (a) Self-doped  $B_{33}H_{32}$  structure, (b) A possible  $H_2$  formation pathway from two adjacent  $B_{33}H_{32}$  layers and (c) Kinetic energy barrier as a function of a reaction path for both self-doped ( $B_{33}H_{32}$ ) and neutral ( $B_{32}H_{32}$ ) structures. Boron is blue (large spheres) and hydrogen is orange (small spheres).

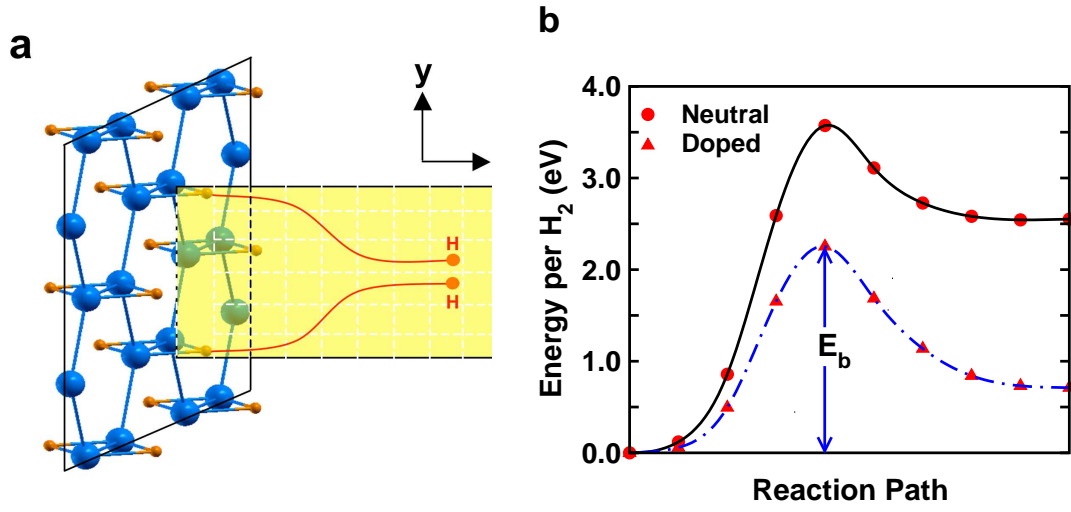


FIG. 4: (Color online) (a) A possible hydrogen release pathway from a single layer  $B_2H_2$  and (b) Kinetic energy barrier ( $E_b$ ) as a function of a reaction path for such a process. Boron is blue (big spheres) and hydrogen is orange (small spheres).

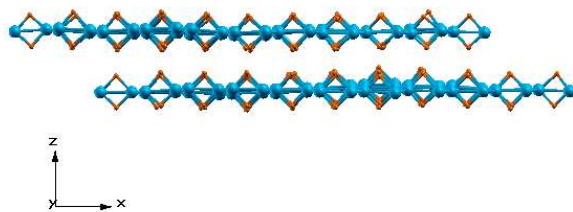


FIG. 5: (Color online) A molecular dynamics simulation snapshot of a neutral  $B_2H_2$  structure. Boron is blue (big spheres) and hydrogen is orange (small spheres).

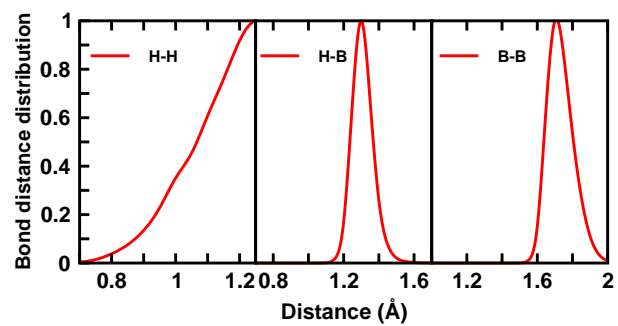


FIG. 6: (Color online) Bond distance distribution for hydrogen-hydrogen, boron-hydrogen and boron-boron, bond distances for a neutral  $B_2H_2$  at a temperature of 500 K.

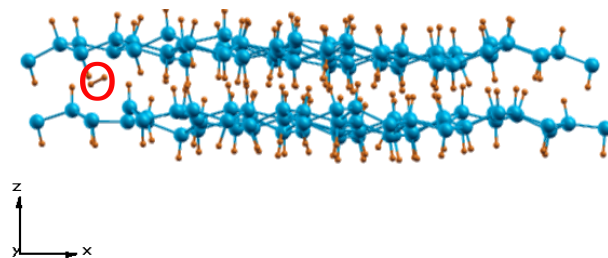


FIG. 7: (Color online) A molecular dynamics simulation snapshot of a charged B<sub>2</sub>H<sub>2</sub> structure which exhibits considerable rearrangements of the H-B bridge bonds and a formation of a H<sub>2</sub> molecule (shown in circle). Boron is blue (big spheres) and hydrogen is orange (small spheres).

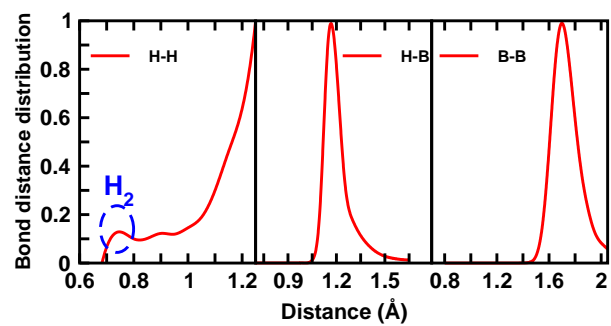


FIG. 8: (Color online) Bond distance distribution for boron-boron, boron-hydrogen and hydrogen-hydrogen bonds for a charged  $B_2H_2$  system at a temperature of 500 K.